JOURNAL OF PROPULSION AND POWER
Vol. 15, No. 6, November–December 1999

Scope of Capacitive Methods in Solid Propellant Diagnostics

U. Carretta,* R. Dondé,† and C. Guarnieri‡
Consiglio Nazionale delle Ricerche–Istituto per la Tecnologia dei Materiali e dei Processi Energetici, 20125 Milan, Italy

Apparatus for instantaneous regression rate measurements based on a simple plane-capacitor geometry and circuit theory is described, and results from a prototype setup are presented for both metallized and nonmetallized AP composite propellants at $p \approx 1$ bar. The experiments show the apparatus is potentially effective as an instantaneous burning rate diagnostic only for the nonmetallized composite propellant. For metallized propellants the technique offers potential as 1) a go/no-go technique and 2) a monitor for the onset of bulk activity inside the gaseous part of the flame. Some tentative general conclusions about the applicability of electric field diagnostics for solid propellants are suggested.

Nomenclature

A, H, D	= capacitor arm width, height, and distance, respectively, cm
a, h, c	= strand width, height, and thickness, respectively, cm
C_a	= parasitic capacity of the neutralization inductance L_a, cm
C_c	= parasitic capacity due to the real layout of the diagnostic chain, cm
$C_f(\omega, t)$	= flame contribution to the capacity, identical to $C_{f1}(\omega, t) - iC_{f2}(\omega, t)$, cm
C_L	= parasitic capacity of the measure inductance L, cm
$C_m(t)$	= capacity of the measure capacitor in the absence of the flame, cm
C_p	= total parasitic capacity at the measure point, $(C_c + C_L + C_a + C_v)$, cm
$C_t(\omega, t)$	= total capacity at the measure point, $[C_m(t) + C_f(\omega, t) + C_p]$, cm
C_v	= parasitic capacity due to the coupling with the vessel, cm
L, L_a	= measure inductance and neutralization inductance, respectively, (s^2/cm)
Q_M	= quality factor of the diagnostic chain at ν equal to ν_M
q_{aM}, q_{LM}	= quality factors of the inductances L_a and L, respectively; $[\omega_M L_a(\nu_M)/R_a(\nu_M)]$ and $[\omega_M L(\nu_M)/R_L(\nu_M)]$, respectively
R_a, R_L	= resistance values of the inductances L_a and L, respectively, (s/cm)
$R(\omega, t)$	= frequency response function of the circuit, $\lvert\Psi_m/\Psi_a\rvert$
$\Re$	= capacity resolving power, $(\eta/\lvert\Delta\eta\rvert_{\min})_{\substack{\eta=1\\ \zeta=0}}$
β	= neutralization fraction, $0 \le \beta < 1$
$\lvert\Delta\eta\rvert_{\min}$	= rms error, identical to $\sqrt{\langle(\Delta\eta)^2\rangle}$
$\varepsilon_s(\omega)$	= dielectric function of the propellant
$\zeta(\omega, t)$	= imaginary part of the nondimensional capacity, $C_{f2}(\omega, t)/[C_m(0) + (1-\beta)C_p]$
$\eta(\omega, t)$	= real part of the nondimensional capacity, $[C_m(t) + C_{f1}(\omega, t) + (1-\beta)C_p]/[C_m(0) + (1-\beta)C_p]$
ν_{ac}, ν_{Lc}	= cutoff frequency values of the inductances L_a and L, respectively, Hz
ν_M	= working frequency value, Hz
$\Phi_a(t), \Phi_m(t)$	= applied voltage and measured signal (statvolt), respectively, $\Phi_{a0}\cos\omega t$ and $\Phi_{m0}(t)\sin[\omega t + \varphi(t)]$, respectively
$\varphi(t)$	= phase difference of $\Phi_m(t)$ with respect to $\Phi_a(t)$, rad
$\Psi_a(\omega)$	= Fourier transform of $\Phi_a(t)$
$\Psi_m(\omega, t)$	= Fourier transform of $\Phi_m(t)$
ω_M	= $2\pi\nu_M$

I. Introduction

THE objective of this work is to examine a plane-capacitor deflagration rate measurement method for solid propellants. This approach is a length measurer and, therefore, possesses all of the difficulties relevant to the burning surface roughness and its inhomogeneous chemical composition. Because the length measurer returns a unique length, an averaging process, depending on the burning's surface roughness and chemical inhomogeneity, implicitly occurs. In quasi-steady situations, that is, when the statistics are time invariant, this is not a problem. However, for nonsteady combustion, the burning surface's roughness and chemical inhomogeneity change, thus confounding the length measurement with the burning surface's statistics and chemical inhomogeneity evolutions.

Because the majority of energetic material applications involves heterogeneous materials, a decisive challenge is to provide accurate and robust instantaneous mass deflagration measurements. The mass deflagration rate is a primary characteristic of any energetic material, and the ability to characterize it accurately in both steady and nonsteady environments is of crucial importance. Nevertheless, this challenge has not been met even though attempts have been made for roughly four decades. Therefore, a multiplicity of concurrent diagnostics may be required. In this context, the simplicity and low cost of the capacitive method make it attractive. Moreover, because differential capacitive measurements can be readily made with bridge circuits, there is potential for direct deflagration rate difference measurements.

The basic ideas of the capacitive method are well known, and very early attempts are described in the literature.[1,2] In practice, a very careful analysis of both the competitive phenomena and circuitry factors affecting the measurement must be performed, to ensure an acceptable reliability. The preliminary experimental data presented in this paper, related to a stationary regime $p \le 1$ bar, are concerned with the measurement of the real and imaginary parts of the complex capacity $C_t(\omega, t)$ of the system. These results offer insight about both the overall scope of capacitive methods and the difficulties to be overcome.

Received 7 February 1998; revision received 20 July 1998; accepted for publication 16 September 1998.

*Senior Researcher, 53 Via R. Cozzi.
†Researcher, 53 Via R. Cozzi.
‡Assistant Researcher, 53 Via R. Cozzi.

II. Experimental Setup

A burning strand of solid propellant is inserted into the plane capacitor, as shown in Fig. 1. The capacitor arms are at a distance $D \approx 20$ mm, their typical dimensions are $A = 20$ mm and $H = 50$ mm. Referring to its equivalent circuit, if L_a represents the inductive branch added to neutralize the parasitic capacities, the Fourier transform $\Psi_m(\omega, t)$ of the signal $\Phi_m(t)$ recorded at the measure point M is given by

$$\Psi_m = \frac{1 + i\omega R_L C_L - \omega^2 L C_L}{1 + i\omega(R_L + i\omega L)C_t(\omega, t) + [(R_L + i\omega L)/(R_a + i\omega L_a)]}\Psi_a \tag{1}$$

This equation is valid provided that $\tau_m \gg 2\pi/\omega$, where $2\pi/\omega$ is the characteristic time-scale of the applied voltage $\Phi_a(t) = \Phi_{a0}\cos\omega t$, and τ_m is the characteristic time of the macroscopic processes, that is, the smallest fluid dynamic time.

In Eq. (1), the total capacity C_t of the circuit includes three contributions: the contribution C_m of the measure capacitor containing the strand acting as a dielectric material, the capacity C_f due to the ionized gaseous phase of the flame, and the total parasitic capacity C_p. For the total parasitic capacity value, for convenience we set $C_p = C_L + C_a + C_v + C_c$, that is, the overall circuit parasitic capacity at the measure point M is split into the sum of four terms. In particular, C_v evidences the coupling of the measure capacitor with the vessel and could be important under high-pressure regimes, where the vessel dimensions are presumably reduced. C_c is the parasitic contribution originating from the physical setup of the circuit, for example, real layout of components into the pads, presence of cables, etc. All of these spurious contributions must be minimized.

The aim of the inductive branch L_a is the neutralization of a β fraction of the total parasitic capacity C_p so that the influence of the bias $C_p \gg C_m(0)$ is reduced.

It is useful to introduce the nondimensional quantities η and ζ, which are the real and the imaginary parts, respectively, of the nondimensional total capacity,

$$\eta(\omega, t) = \frac{C_m(t) + C_{f1}(\omega, t) + (1 - \beta)C_p}{C_m(0) + (1 - \beta)C_p}$$

$$\zeta(\omega, t) = \frac{C_{f2}(\omega, t)}{C_m(0) + (1 - \beta)C_p}$$

Notice that there is a flame contribution $C_{f1}(\omega, t)$ to the real part η, whereas the imaginary part ζ is entirely due to the flame. The details of the behavior of the measuring circuit, related equations, constraints, design specifications, in-situ determination of the operative parameters, performances, etc., are all fully described in Refs. 3–5.

To determine η and ζ, the observable quantities are the amplitude $\Phi_{m0}(t)$ and phase $\varphi(t)$ of the signal recorded at point M of Fig. 1: $\Phi_m(t) = \Phi_{m0}(t)\sin[\omega t + \varphi(t)]$. Measurements were performed at a fixed angular frequency value (the working frequency) $\omega_M = 2\pi\nu_M$ for which the response function $|\Psi_m/\Psi_a|$ of the circuit is maximum,

$$\omega_M = \omega_{ro}\sqrt{1 + \frac{L}{L_a}} \equiv \sqrt{\frac{1}{L[C_m(0) + (1 - \beta)C_p]}} \tag{2}$$

where $\omega_{ro} = \sqrt{\{1/[L(C_m(0) + C_p)]\}}$ gives the maximum of the response function if there were no added inductance L_a.

The operative parameters of the homemade measuring circuit used are: $L = 45.92\,\mu\text{H} \pm 1\%$ and $L_a = 21.02\,\mu\text{H} \pm 1\%$; their cutoff frequencies are $\nu_{Lc} = 20.20$ MHz and $\nu_{ac} = 23.90$ MHz, respectively. From the cutoff frequencies, $C_L = 1.35$ pF and $C_a = 2.11$ pF are derived. At $\nu_M \cong 14.5$ MHz, for the quality factors of the inductive branches shown in Fig. 1, one finds: $q_{LM} = 33.2$ and $q_{aM} = 27.4$, so that an overall quality factor Q_M of the circuit can be defined,

$$\left|\frac{\Psi_m}{\Psi_a}\right|_{\max} \equiv Q_M \approx \frac{q_{LM}}{1 + (q_{LM}L/q_{aM}L_a)}\left(1 - \left(\frac{\nu_M}{\nu_{Lc}}\right)^2\right) \approx 4$$

To evaluate the (spatial) resolving power, one must calculate $\Delta\eta = (\partial\eta/\partial R)\Delta R + (\partial\eta/\partial\varphi)\Delta\varphi$. For a signal $\Phi_m(t) = \Phi_{m0}(t)\sin[\omega t + \varphi(t)]$, on the fast timescale $\tau = 2\pi/\omega$ it is straightforward to find that $\Delta\varphi$, at the best, is equal to ΔR. Thus, we set $\Delta\varphi \approx \Delta R$ and calculate the rms error $|\Delta\eta|_{\min} \equiv \sqrt{\langle(\Delta\eta)^2\rangle}$ at $\eta = 1, \zeta = 0$, that is, in the absence of the flame. The capacity resolving power $\Re$ is given by

$$\Re = \left(\frac{\eta}{|\Delta\eta|_{\min}}\right)_{\substack{\eta=1\\ \zeta=0}} = \frac{Q_M^2}{|\Delta R|_{\min}} \approx \frac{16}{|\Delta R|_{\min}} \tag{3}$$

where $|\Delta R|_{\min}$ is the rms error in the detected amplitude ratio, that is, is the smallest detectable variation of R. These results hold disregarding the terms of $\mathcal{O}(1/q^2)$ or $\mathcal{O}[(\nu_M/\nu_{Lc})^4]$ in the related equations.

From a direct measurement of the total noise (see Fig. 2), one finds $|\Delta R|_{\min} \approx 5.5 \times 10^{-3}$ and $\Re \cong 2900$. From the expressions of η at $C_f = 0$ and $\Re$ [see Eq. (3)], in the plane-capacitor approximation one can calculate $|\Delta h|_{\min}$, the smallest detectable variation of the strand height

$$|\Delta h|_{\min} = \frac{4\pi}{L\omega_M^2}\left(\frac{D}{a}\right)\frac{1}{\Re}\frac{1 - (c/D)[1 - (1/\varepsilon_s)]}{(c/D)[1 - (1/\varepsilon_s)]} \tag{4}$$

Of course, the flame contribution strongly affects this figure of merit.

In dealing with solid propellants, some considerations about Eq. (4) are required. The first term $1/(L\omega_M^2)$ evidences the requirement for a good neutralization of the parasitic capacity [see Eq. (2)]; the term D/a is not critical, it can be reduced not far from 1 by means of a suitable choice of the system dimensions; the most critical parameter is the transverse filling ratio c/D. In practice, the tradeoff is between the requirement of an effective filling of the capacitor and

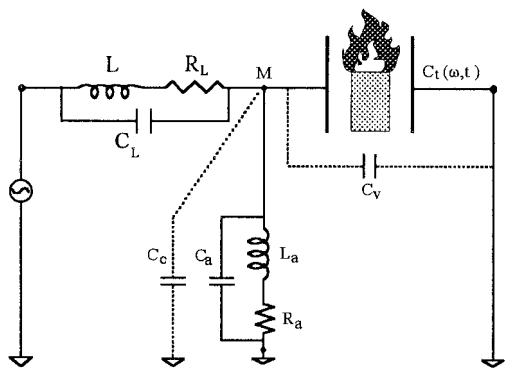

Fig. 1 Sketch of the equivalent circuit for the diagnostic chain.

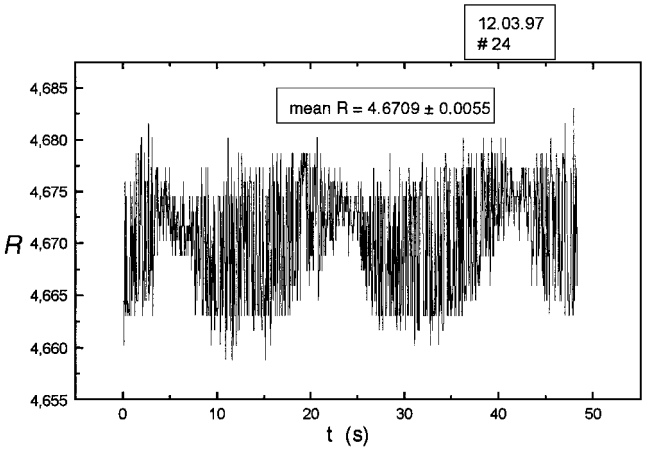

Fig. 2 Time recording of the response function *R*.

the necessity of preventing the interaction of the flame with the capacitor arms. This interaction strongly affects the heat balance of the process, and therefore, a good nonconductive coating is required.

The presence of an insulating coating for the capacitor arms is mandatory for avoiding the collection of the conduction current from the flame: a requirement that could not be fulfilled by the unsuitable layout of earlier experiments.[1,2]

To obtain a figure of merit for the case in consideration, by assuming $c/D = 0.5$ and $\varepsilon_s = 2$, one obtains $|\Delta h|_{\min} = 890(D/a)(1/\Re)$ mm. Because the aforementioned value for the capacity resolving power $\Re = 2900$ was achieved by using a rough homemade wide-range frequency generator, a $|\Delta h|_{\min}$ of the order of 10 μm is not beyond the scope of the proposed technique.

Finally, in regards of the neutralization coefficient β one gets

$$\beta = \frac{C_m(0) + C_p}{C_p} \cdot \frac{L/L_a}{1 + L/L_a} \cong \frac{L/L_a}{1 + L/L_a} \cong 68\%$$

The higher is $\beta < 1$, the lower is $|\Delta h|_{\min}$. The value 68% for the prototype can obviously be increased by a better choice of the coils L and L_a. This value results solely from the necessity of using two home-available, ready-for-use coils of proper values, in order to avoid exceeding the frequency capability of the input generator [see Eq. (2)].

III. Experimental Results

Propellant strands of AP.HTPB/86.14, with cross section 7×12 mm and height $h \sim 60$ mm, were inserted into the plane capacitor with arms set at $D = 22$ mm. The typical $\eta(t)$ and $\zeta(t)$ histories are shown in Figs. 3 and 4, respectively. The filling ratio in the direction perpendicular to the arm surfaces is $\frac{7}{22} = 0.318$. The arms are coated with an insulating material to prevent the collection of conduction current; ceramic coatings such as Ceramabond adhesives behave properly. Figures 3 and 4 also show the pressure history.

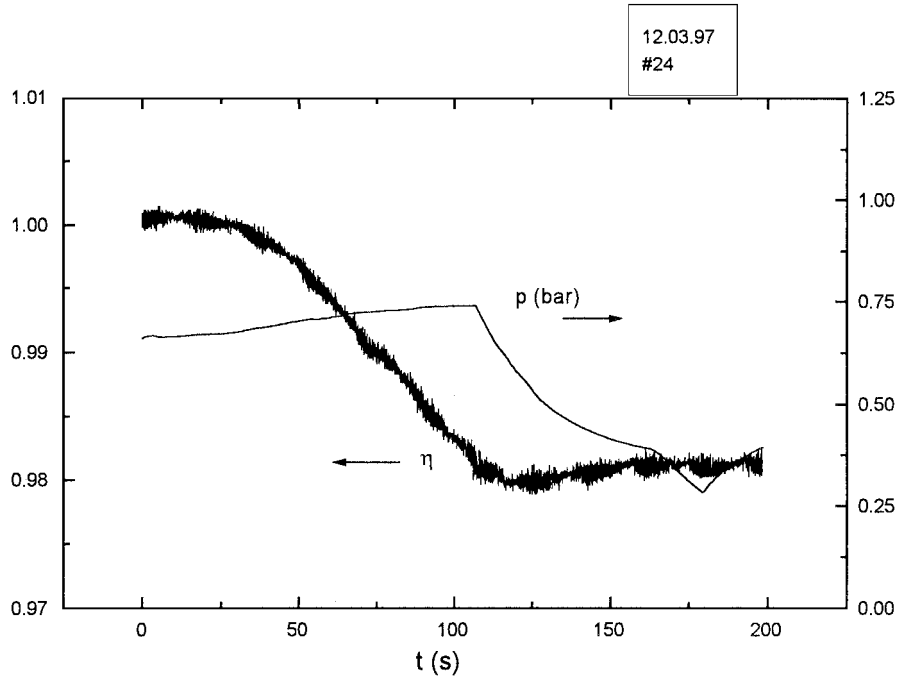

Fig. 3 Evolutions of the real part η of the non-dimensional capacity and of the pressure p during the burning of an AP.HTPB/86.14 propellant strand at $p < 1$ bar.

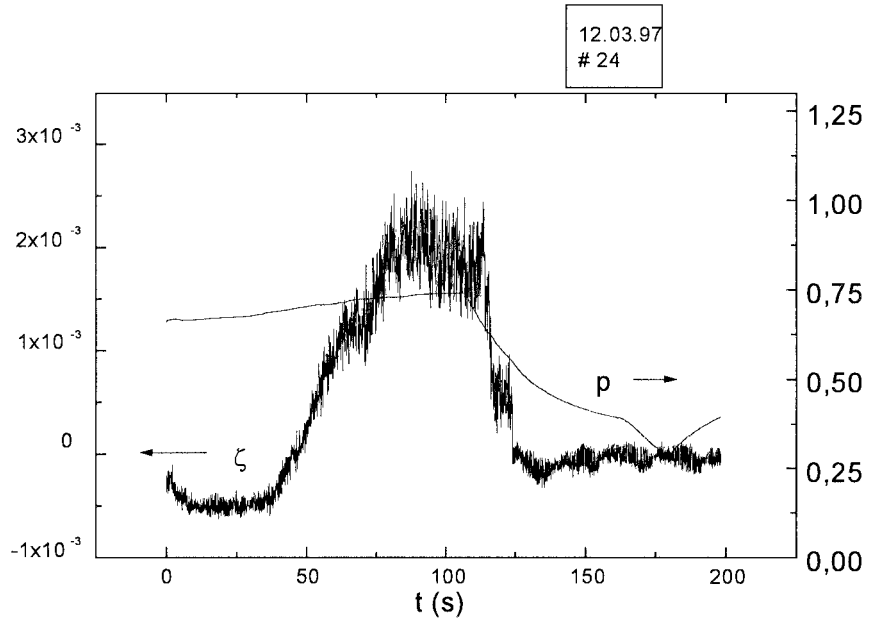

Fig. 4 Evolutions of the imaginary part ζ of the non-dimensional capacity and of the pressure p during the burning of an AP.HTPB/86.14 propellant strand at $p < 1$ bar.

The $\eta(t)$ history is well behaved, as evidenced by the presence of the decreasing linear portion once the border effects have became negligible (border effects are better revealed in a subsequent figure). In fact, the strand is ~10 mm taller than the upper bound of the capacitor arms in order to accomplish ignition. This also assesses the acceptability of the infinite plane-capacitor approximation.

The influence of the flame seems to be negligible, as also suggested by the low $\zeta(t)$ values. This result is primarily due to the working frequency value, higher than the one used in Refs. 3 and 4 where, in addition, there was no neutralization of the parasitic capacity C_p. In fact, the higher the working frequency is, the lower is the flame contribution to both the real and the imaginary parts of the capacity.

A simple test-particle model[3,4] for the flame conductivity led to the trivial conclusion that the dominant quantity is the conductivity parameter $\omega_p^2/(\omega_M \overline{\nu_c})$, where ω_p is the plasma frequency of the ionized portion of the flame and $\overline{\nu_c}$ an average collision frequency of the charge carrier population (this result holds in collisional regimes when $\nu_M \ll \overline{\nu_c}$). Moreover, when $\omega_p^2/(\omega_M \overline{\nu_c}) \gg 1$, a simple model,[5] assuming a Lorentzian shape for the space profile of the ionization inside the flame along the longitudinal direction, that is, parallel to the capacitor arms, shows that the real and imaginary parts of the flame contribution to the total capacity are of the same order: $C_{f1}(\omega, t)/C_{f2}(\omega, t) = \mathcal{O}(1)$.

By observing the expression of the conductivity parameter, in addition to the increase of the working frequency, an increase of the average collision frequency should be effective in quenching the flame contribution to the capacity, at least for low-ionization flame where most of the collisional events are with neutrals. Because any reliable prediction of the partial fraction equilibrium inside the flame is difficult, experimental work at different pressures is required to clarify this point, especially with respect to the possibility of performing experiments with fast pressure transients.

The situation is different when burning the metallized propellant AP.HTPB.Al/68.14.18: The flame contribution completely masks the regression of the solid (see Fig. 5). In this run, the independence of pressure from burning is questionable, despite the large vessel volume, as evidenced by the final burst before extinction when the combustion becomes volumetric. Direct comparison of η and ζ confirms the dominance of the gaseous portion of the flame: They have almost the same evolution (see Fig. 6). Notice that the η behavior suggests a flame profile rather close to the burning surface and

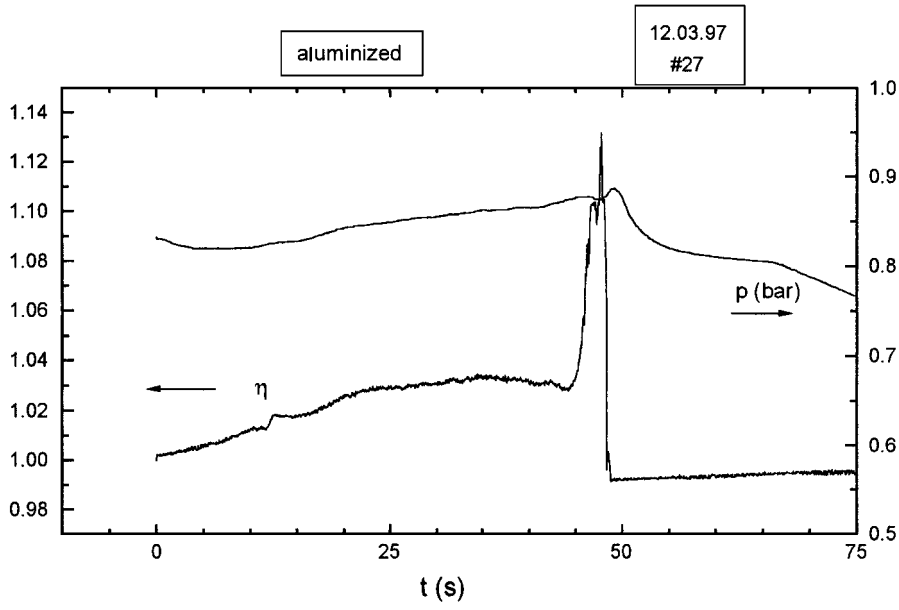

Fig. 5 Same as in Fig. 3 for a metallized propellant strand: AP.HTPB.Al/68.14.18.

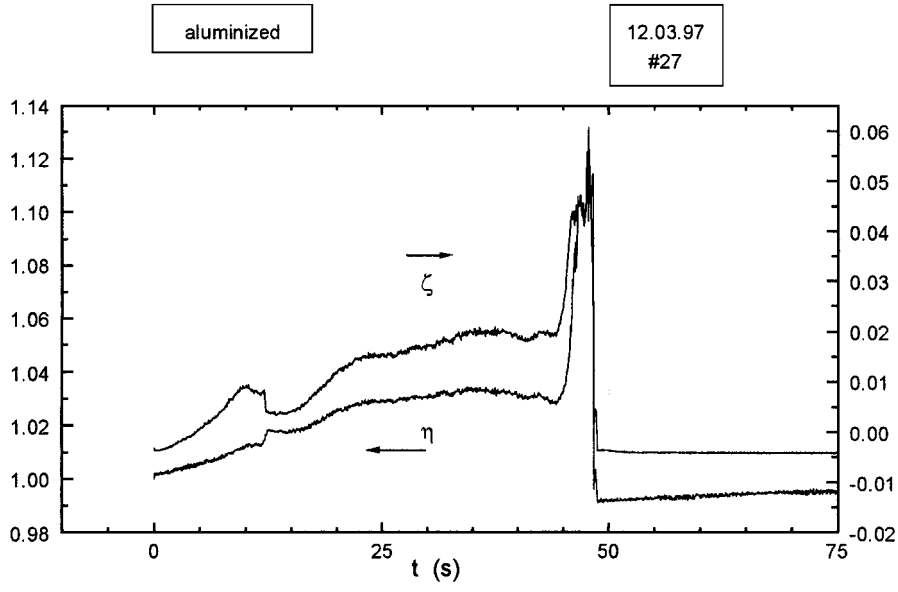

Fig. 6 Comparison between η and ζ for the run presented in Fig. 5.

spatially broad in the longitudinal direction away from the burning surface.[6]

IV. Experimental Considerations

The representative low-pressure results reported for the nonmetallized propellant require two observations.

First, from frequency measurements and Eq. (2), the total capacity C_t can be determined in three different situations: C_{tv} (v for vacuum) is the value when the measure capacitor is empty, C_{t0} is the value when the propellant strand is into the capacitor just before the beginning of the burning (the ready-to-start situation) and, eventually, $C_{t\infty}$ is the value after the end of the burning. For the case shown in Figs. 3 and 4, one gets $C_{tv}/C_{t0} = 0.989$ and $\eta_v = C_{tv}/C_{t0} - (L/L_a)(1 - C_{tv}/C_{t0}) = 0.965$ due to the partial neutralization of the bias C_p. Figure 3 shows that $\eta_\infty \cong 0.98 > \eta_v$, that is, $C_{t\infty} > C_{tv}$, and, moreover, the capacity shows a very slow but observable increase.

More refined experimental work is needed to reach a definite assessment about the influence of the deposition of ashes inside the measurement chamber, especially in the neighborhood of the capacitor arms, where a short circuit would dangerously affect the whole measurement. From this point of view, better results are expected from high-pressure regimes, where the combustion process is upgraded. Similar care must be devoted to the overall fluid dynamics of the chamber (especially with respect to the combustion effects on pressure stability) and to the occurrence of thermomechanical deformations of the measure capacitor.

A second point of discussion results from the observation that the ζ evolution at the beginning of the combustion shows negative values, despite that, according to the formalism developed, ζ is a positive-definite quantity. Although a small negative bias for ζ in a neighborhood of 0 can result from the numerical code that elaborates the recorded amplitude and phase values (the test program for the numerical algorithms used gives $\zeta = -10^{-7}$ for the given value $\zeta = 0$), the negative behavior of ζ at the early times of combustion is well beyond this order of magnitude and, moreover, is repetitive. This fact is not clear, and further observations are required, especially about the influence of the dc-biased hot ignition wires.

V. Determination of the Regression Rate

When $\eta(t)$ is known and the flame contribution C_{f1} to the real part of the capacity is negligible, one obtains

$$\frac{d\eta}{dt} = \frac{1}{C_m(0) + (1-\beta)C_p}\frac{dC_m(t)}{dt} = K\frac{dh(t)}{dt}$$

where $h(t)$ is the height of the strand into the measure capacitor and K an overall quantity that, in the plane approximation, can be considered constant.

Of course, from an operative point of view, this is strictly true only provided the proper disposition of guard capacitors is used, thus involving the experimental situation. Otherwise, in a rigorous description of a real, that is, finite, plane capacitor, for example, by any of the usual codes, the regression of a dielectric strand between the arms is a three-dimensional effect that (depending on dimensional ratios) can be considered constant only in a fraction of the longitudinal extension of the capacitor itself. Only in this more or less broad region, K can be considered constant.

In spite of these considerations, which suggest rigorous procedures for improving the reliability of the method, the η evolution evidenced in Fig. 3 is so well behaved that, as a first step, K can be approximately determined by a simple comparison with the regression rate measured under stationary conditions by means of other methods, for example, by the usual optical inspection. The determined K value is related not only to the strand material, but also to the specific experimental setup for the capacitor arms and the strand dimensions used in the stationary regime. Once K is known, $d\eta/dt$ also yields the regression rate under nonsteady conditions.

The preceding observations are confirmed by the results summarized in Fig. 7, where, for instance, the pressure is a little higher (and a little more stable) than in the preceding case. Here, the ash effect and slow η increase after the extinction are worse, because $\eta_v = 0.974$.

In spite of these considerations, even a closer insight of the η evolution, for example, that of the unlucky run presented in Fig. 7, shows a well-defined linear behavior. This soundly suggests the possibility of determining the earlier mentioned constant K (see Fig. 8). To do this, one can compare the η evolution of Fig. 8 with the video-camera recording of the burning surface position, as shown in Fig. 9 by the heavy dots. The horizontal dotted lines indicate the upper and the lower boundaries of the capacitor arms. Disregarding the first and the last seconds of the burning, when border effects dominate the η evolution, both the surface position and η show a linear time behavior, thus assessing the acceptability of the plane-capacitor approximation. In fact, according to this assumption, the nondimensional capacity η is a nonincreasing linear function of the position (although, trivially, the straight lines cannot be the same).

From Fig. 9, at $t = 77$ s the burning surface is at about one-half of the arm extension. By averaging the data for η of Fig. 8 around this value of t, for example, between $t = 60$ and 90 s, and calculating the regression rate from the video-camera data, we can obtain $d\eta/dt$ and then K. The regression rate calculated from the video-camera data is shown in Fig. 10. The average value between $t = 60$ and 90 s is $r_b \cong 7.15 \times 10^{-2}$ cm/s. From this value and $d\eta/dt \cong -1.8 \times 10^{-4}$ s^{-1}, the value $K \cong 2.52 \times 10^{-3}$ cm^{-1} is found.

Let us summarize the rationale of the technique. In the simple plane-capacitor geometry presented, the implemented method can,

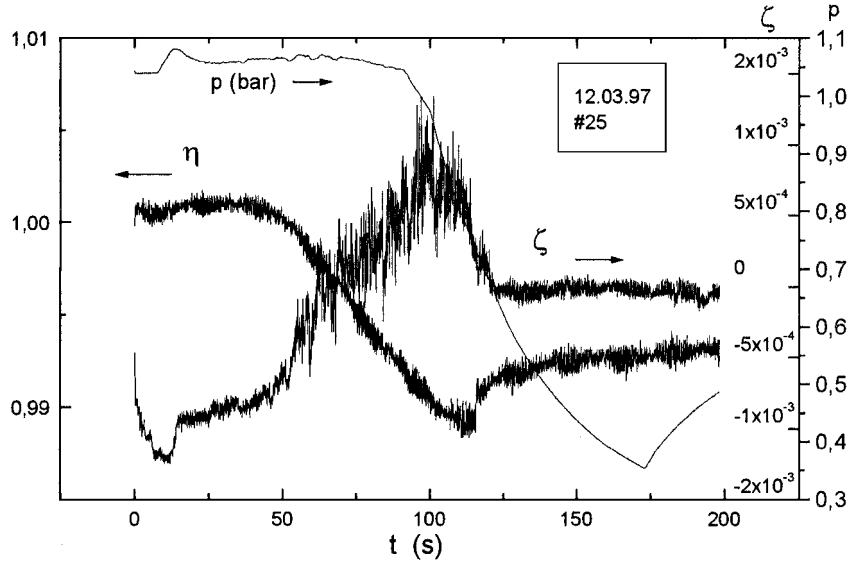

Fig. 7 Time evolutions of η, ζ and pressure p during the burning of an AP.HTPB/86.14 propellant strand at $p \cong 1$ bar.

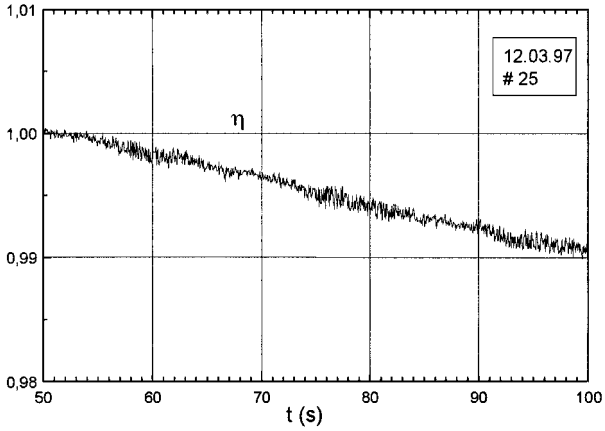

Fig. 8 Time evolution of η between $t = 50$ s and $t = 100$ s for the run of Fig. 7.

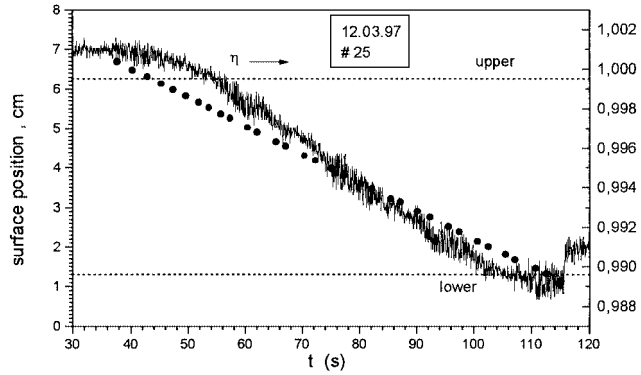

Fig. 9 Comparison between the η evolution and the burning surface position (●) during the run presented in Fig. 7. · · · · ·, the upper and the lower boundaries of the capacitor arms.

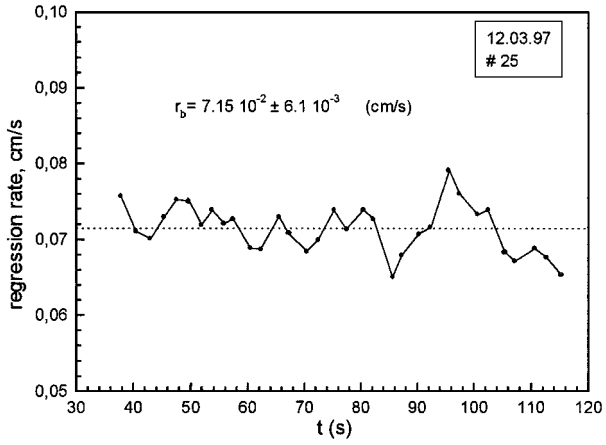

Fig. 10 Regression rate r_b calculated from the burning-surface position recorded in Fig. 9.

in principle, detect the position in time of a boundary surface separating two media with appreciably different dielectric function values. Therefore, if the dielectric function values ε_1 and ε_2 are known, if these functions are spatially uniform in each of the regions bounded by the surface, and if this surface always remains perpendicular to the capacitor arms during its motion, a simple numerical code can solve the problem.

For solid propellants the reality is very different. Even in the condensed phase the dielectric function is unknown, due to various phenomena triggered, for example, by the thermal wave. This scenario becomes worse in the gaseous part of the flame, which often is a true multiphase region including not only a ionized portion, but also

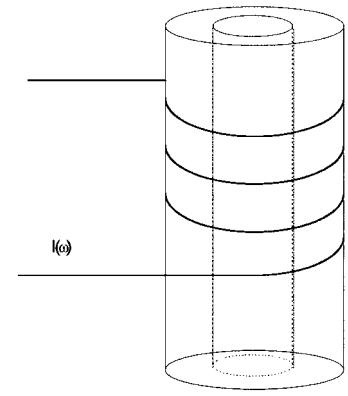

Fig. 11 Conceptual sketch of a propellant grain "wired" by a solenoid: the magnetic flux expulsion due to the high conductivity of the ionised gas inside the burning cavity modifies the inductance of the system.

oxidizer particles, metal particles, ashes, etc., making any theoretical description extremely difficult. Moreover, the burning surface is a more or less extended region of great complexity, and our conceptual idealization often fails to meet the reality. A noticeable contribution in this area, well beyond the limits of this coarse-grained propellant discussion, is given in Ref. 7. Although addressed to play on a different and broader scenario, the contribution also provides useful hints to experimentalists.

In the authors' opinion, all of these difficulties can affect the reliability of this simple and cheap technique to an extent not greater than that affecting most of the other techniques aimed to measure length in solid propellant diagnostics. Moreover, this method, which in principle detects a process front, also can operate with porous systems, that is, with systems where the apparent shape of the matrix does not change, so that, for instance, optical methods are useless. The preliminary data presented cannot claim the rank of systematic investigation; they simply act as useful specimens to investigate the overall scope of the technique. Therefore, no comparison with the data of other existing techniques is now suggested. Of course, the proposed technique also is being used at higher pressures ($p \approx 50$ bar) and under pressure transients, but this is another work.

VI. Conclusions

The performances of the homemade prototype diagnostic circuit seem to assess the effectiveness and reliability of this simple electrostatic method in detecting even small capacity variations. Nevertheless, the results collected at a fixed working frequency ν_M show the following.

1) For nonmetallized propellants, the method seems to achieve the goal, although a large amount of experimental work is required to definitely assess its reliability at higher pressures, especially under unsteady regimes and with respect to the remarks discussed in the preceding section.

2) For metallized propellants, the capacitor method is unable to detect the regression of the burning surface, due to the exceedingly high conductivity of the flame with respect to the working frequency. In this case, the method merits use as a very sensitive detector in go/no-go experiments or for monitoring the onset of gross instabilities inside the flame.

The difficulties encountered with the metallized propellants will affect the reliability of any electric method concerned with either the longitudinal or the transverse electric field (such as in μ-wave techniques). Unless the working frequency is so high that, for instance, the ionized component of the gaseous portion of the flame becomes transparent to the pump, the way toward the x-ray region seems to be mandatory. Another, rather exotic approach, based on the high conductivity of the flame, could be as shown in Fig. 11.

In cylindrical geometry, the high conductivity of the expanding inner region inside a burning propellant grain causes magnetic field expulsion, thereby varying the geometric inductance of the excitation coil. Can this variation, if detectable, be clearly correlated to the (more or less axisymmetric) radial regression of the solid surface, despite the activity inside the ionized phase (conductivity variations, modes, turbulence, etc.)?

Finally, an interesting question is the following: If the conductivity of the gaseous portion of the flame for metallized propellants is so high, can a proper layout of magnetic pickup coils (along, for example, the rocket motor) detect the magnetic field perturbations related to the onset of dangerous modes inside? In principle, electrostatic tomography also could offer substantial information about the behavior of both the propellant and the gaseous phase inside the motor. Of course, a suitable test motor is required, together with the necessary point sources for the excitation currents and/or potentials.

Acknowledgments

Financial support under Consiglio Nazionale delle Ricerche-Agenzia Spaziale Italiana Contract ARS-96-13 Proposal 396/2/SIN is acknowledged. The authors also gratefully acknowledge P. Giuliani for his technical assistance. Finally, the authors must be thankful to all the Referees, especially to the very patient and anonymous one whose fruitful criticism greatly enhanced the authors' scientific consciousness.

References

[1]Hermance, C. E., "Continuous Measurement of the Burning Rate of a Composite Solid Propellant," *AIAA Journal*, Vol. 5, No. 10, 1967, p. 1775.

[2]Yin, C. F., and Hermance, C. E., "Continuous Measurement of Transient Burning Rates of a Composite Propellant Undergoing Rapid Depressurization," AIAA Paper 71-173, Jan. 1971.

[3]Carretta, U., Colombo, G., and Guarnieri, C., "Electrostatic Method for the Instantaneous Burning Rate Measurement in Solid Materials," Consiglio Nazionale delle Ricerche-cnpm Activity Rept., Sept. 1992.

[4]Carretta, U., Giuliani, P., Guarnieri, C., and Zanotti, C., "Electrostatic Method for the Instantaneous Burning Rate Measurement in Solid Materials," 25th International Symposium on Combustion, Paper WIP-25-212, Univ. of California, Irvine, CA, July–Aug. 1994.

[5]Carretta, U., and Guarnieri, C., "Upgraded Diagnostic Chain for the Burning Rate Measurement in Solid Materials," Consiglio Nazionale delle Ricerche-cnpm Activity Rept., Sept. 1995; also INTAS Workshop, Combustion of Advanced Energetic Materials, Politecnico di Milano, Milan, Italy, July 1996.

[6]Zanotti, C., Carretta, U., Grimaldi, C., and Colombo, G., *Nonsteady Burning and Combustion Stability of Solid Propellants*, edited by L. DeLuca, E. W. Price, and M. Summerfield, Vol. 143, Progress in Astronautics and Aeronautics, AIAA, Washington, DC, 1992, p. 419.

[7]Glick, R. L., Fisher, M., and Miller, R. R., "On Nonsteady Burning of Heterogeneous, AP Like Propellants," International Workshop on Combustion Instability of Solid Propellants and Rocket Motors, Politecnico di Milano, Milan, June 1997.